Chemical Physics Letters 504 (2011) 83–87

Contents lists available at ScienceDirect

Chemical Physics Letters

journal homepage: www.elsevier.com/locate/cplett

Resonant neutral particle emission in collisions of electrons with protonated peptides with disulfide bonds at high energies

Tetsumi Tanabe [a,b,*], Koji Noda [b], Satoshi Miyagi [c], Noriyuki Kurita [c], Shigenori Tanaka [d], Julia Setzler [e], Wolfgang Wenzel [e], Evgeni B. Starikov [f,g,h], Gianaurelio Cuniberti [f,g]

[a] High Energy Accelerator Research Organization (KEK), Accelerator Laboratory, 1-1 Oho, Tsukuba, Ibaraki 305-0801, Japan
[b] Department of Accelerator and Medical Physics, National Institute of Radiological Sciences, Anagawa, Chiba 263-8555, Japan
[c] Department of Knowledge-based Information Engineering, Toyohashi University of Technology, Tenpaku-cho, Toyohashi 441-8580, Japan
[d] Graduate School of System Informatics, Department of Computational Science, Kobe University, 1-1 Rokkodai, Nada, Kobe 657-8501, Japan
[e] Institute for Nanotechnology, Karlsruher Institut für Technologie (KIT), P.O. Box 3640, 76021 Karlsruhe, Germany
[f] Institute for Materials Science, Technical University of Dresden, 01062 Dresden, Germany
[g] Division of IT Convergence Engineering, POSTECH, Pohang, South Korea
[h] Department of Physical Chemistry, Chalmers University of Technology, SE-412 96 Gothenburg, Sweden

ARTICLE INFO

Article history:
Received 30 September 2010
In final form 21 January 2011
Available online 26 January 2011

ABSTRACT

Electron–ion collisions were studied for various protonated peptide monocations with disulfide bonds, using an electrostatic storage-ring equipped with a merged-electron-beam device. Resonant neutral particle emissions at the energies of 6–7 eV were observed, as well as a rise towards zero-energy, which are typical electron-capture dissociation profiles. The presence of disulfide (S–S) bonds tends to enhance the resonant bump heights. Chemical nature of the amino-acid residues adjacent to cysteines appears to correlate with the bump strength. Molecular-dynamical simulations help clarify the role of molecular vibration modes in the electron-capture dissociation process.

1. Introduction

Molecular dissociations in collisions of cations with electrons have attracted much interest both in atomic physics [1,2] and in biomolecular science [3]. They are called the dissociative recombination (DR) and the electron-capture dissociation (ECD) in the former and the latter, respectively. Both are similar concepts, but DR leads to the breakage of small molecules like diatomics, while ECD predominantly causes the cleavage of biomolecular bonds. The DR and ECD have been known to occur at very low collision energies. The ECD on multiply-protonated peptides was first found to cleave N–C_α bond [3] in mass spectrometry experiments. Furthermore, it was also clarified that disulfide bonds in multiply protonated proteins are preferentially cleaved by low-energy electrons [4]. Since then, the ECD which leads to both backbone and S–S bond cleavages has extensively been studied both experimentally and theoretically [5–34]. The following mechanisms on the ECD have been proposed: Electron capture is postulated to occur initially at a protonated site to release an energetic hydrogen atom that is captured at high-affinity site such as S–S or backbone amide to cause nonergodic dissociation [5]. Meanwhile, charged peptides with alkali cations such as Li^+ and Na^+ instead of protons also show the ECD features in collisions with electrons, producing the alkalated analogs of c, z ions [30,35]. This means that the protonation is not necessarily required in the ECD fragmentation. Here, it should be noted that unlike protons, which should be covalently bonded to anionic amino-acid residues, alkali cations exhibit non-covalent π–cation interactions with any protein fragment rich in electron density [36,37]. Another mechanism has been proposed that an electron initially is captured into a Rydberg orbital at a positively charged site and subsequently undergoes intra-molecular electron transfer to S–S σ^* or amide π^* orbital to effect the disulfide linkage or N–C_α bond cleavage, respectively [11].

It is well known that ECD is efficient for thermal electrons and the cross sections rapidly decrease with an increase of electron energies. The rate has a maximum at zero energy and drops two to three orders of magnitude at 1 eV. On the other hand, the DR cross sections often exhibit maxima at several tens of electron volts as well as zero energy [1,2]. For ECD, the rate was also found to be significant for high energy (3–13 eV) electrons for polypeptide polycations and is dubbed 'hot electron capture dissociation' (HECD) [6]. The high energy resonance having a maximum at around 6–7 eV was also found in collisions of electrons with singly protonated peptides in the storage-ring experiments [38]. This can also result from the same mechanism. When being captured, a free electron loses its kinetic energy to produce excited electron states which have energies enough for molecular dissociation. In the HECD, not only N–C_α bonds are cleaved, unlike in the ECD, but

* Corresponding author at: High Energy Accelerator Research Organization (KEK), Accelerator Laboratory, 1-1 Oho, Tsukuba, Ibaraki 305-0801, Japan.
E-mail address: tetsumi.tanabe@kek.jp (T. Tanabe).

0009-2614/$ - see front matter © 2011 Elsevier B.V. All rights reserved.
doi:10.1016/j.cplett.2011.01.058

Table 1
Peptide sequences.

Peptide label	Peptide sequence	Peptide label	Peptide sequence
Peptide I (SS)	H-Cys-Val-OH H-Cys-Val-OH	Peptide V (SS) (Vasotocin)	Cys-Tyr-Ile-Gln-Asn-Cys-Pro-Arg-Gly-NH_2
Peptide II (SS)	H-Gly-Cys-OH H-Gly-Cys-OH	(SH)	Cys-Tyr-Ile-Gln-Asn-Cys-Pro-Arg-Gly-NH_2
Peptide III (SS)	H-Cys-Tyr-OH H-Cys-Tyr-OH	Peptide VI (SS) (Vasopressin)	Cys-Tyr-Phe-Gln-Asn-Cys-Pro-Arg-Gly-NH_2
(SH)	H-Cys-Tyr-OH	(SH)	Cys-Tyr-Phe-Gln-Asn-Cys-Pro-Arg-Gly-NH_2
Peptide IV (SS) (Glutathione)	H-Glu(Cys-Gly-OH)-OH H-Glu(Cys-Gly-OH)-OH	Peptide VII (SS) (Oxytocin)	Cys-Tyr-Ile-Gln-Asn-Cys-Pro-Leu-Gly-NH_2
(SH)	H-Glu(Cys-Gly-OH)-OH	(SH)	Cys-Tyr-Ile-Gln-Asn-Cys-Pro-Leu-Gly-NH_2

the excess of energy upon the primary c, z^* cleavage may induce secondary fragmentation in z^* fragments [6,7]. The high-energy resonance has also been found for alkali-metal adducted peptide mono-cations [37] in almost the same energy range.

Still, the high-energy resonances we have reported so far are for the peptides without S–S linkage. Now we would like to report on collisions of high-energy electrons with disulfide-bonded peptide mono-cations to systematically check what is the contribution of the S–S bond cleavage to the over-all HECD mechanism. Our electrostatic-storage-ring experiments allow detection of neutral reaction products under well-defined collision energies, as compared with the FTICR (Fourier Transform Ion Cyclotron Resonance) method widely used, and this is why our data may be an essential addition to the available findings. Besides, for the longer oligopeptides under study, we also theoretically investigate vibrational normal modes which can be relevant to the HECD mechanism. All this helps us gain a further insight into the latter.

2. Experimental

2.1. Materials

Table 1 represents the peptides used in this experiment. The peptides I–III (SS) and IV (SS) are the disulfide linked peptides of two and three amino acid residues, respectively. The peptides V–VII (SS) are composed of nine residues, in which two cysteine residues form an internal disulfide bond. The other peptides shown as (SH) contain cysteines with mercapto (or thiol) group (–SH).

The $(H\text{-}Cys\text{-}Val\text{-}OH)_2$, $(H\text{-}Gly\text{-}Cys\text{-}OH)_2$ and $(H\text{-}Cys\text{-}Tyr\text{-}OH)_2$ peptides (oxidized form) were purchased from Bachem (Switzerland). Glutathiones (oxidized and reduced forms) were purchased from Wako Pure Chemical (Japan). Vasotocin (VT), Vasopressin (VP) and Oxytocin (OXT, oxidized form) were purchased from Peptide Institute (Japan). The SH peptides were obtained by reducing corresponding SS peptides with Tris (2-carboxy ethyl) phosphine HCl (TCEP) purchased from Nacalai Tesque (Japan), except Glutathione.

2.2. Electrospray ion source and injection line

Singly protonated peptides were produced in an electrospray ion source (ESI) from a solution with a biomolecule concentration of about 0.1 mM dissolved in water (50%) and methanol (50%) mixture. A small amount of acetic acid was added to help protonation. Ions produced in the ESI were then conveyed to an octupole ion trap and accumulated there through collisions with helium gas. After storage for about 5 s, ions were ejected as a bunch and accelerated to 20 keV [39]. The ion beam was then mass-analyzed and the selected mono-cations were injected into the storage ring.

2.3. Electrostatic storage ring and electron target

Experiments were performed using an electrostatic storage ring [40] and a merged electron beam [41] with a thickness of about 20 cm. Neutral reaction products were detected by a micro-channel plate (MCP) installed in the vacuum extension outside the ring. Details of the experimental setups and methods have been described in Ref. [38]. The injected ions into the storage ring were first stored for 0.5 s in order to de-excite vibrationally excited ions, and then measurements were started. In order to estimate the background through collisions with residual gas, the electron beam was chopped at a time width of 0.25 s. The stored ion beam gradually decayed with time through collisions with the residual gas. At a time of 5.5 s after injection, the stored ion beam was dumped and renewed at every injection period. The electron acceleration voltage was scanned in small steps.

3. Computational approaches

The longest peptides involved have been studied using molecular-dynamics (MD) and density-functional-theory (DFT) computations to investigate the possible role of molecular vibrations in the ECD process. We employed the B3LYP/6-31G(d,p) method in GAUSSIAN 03 [42] for obtaining stable structures of all these peptide molecules.

The initial-guess structures for *in vacuo* molecular-dynamical (MD) simulations were taken from the results of the above quantum-mechanical (QM) computations. First, for all the three molecules, MD equilibration during 1 ps was performed and then a 3 ns production MD trajectory was generated (the time step was 1 fs for both equilibration and production). Throughout the simulations, the sulfur atoms of the S–S bridges were frozen. Here, the software package AMBER 10 [43] and the force field ff99SB [44] were employed. The simulation temperature was 300 K and the simulation was carried out in microcanonical (NVE) ensemble.

The production MD trajectories thus obtained were interpreted in terms of correlations between Cartesian coordinates of the centers of mass of the respective amino acid residues. The resulting correlation matrices were analyzed to reveal the underlying dynamical domains (collective normal modes (deterministic dynamics) vs. modes which participate in the thermal motion). This type of interpretational approach has been successfully applied to study hydration shells of cyclodextrins and is in detail described elsewhere [45]. One might view our MD trajectory processing approach as a specific hybrid between Essential Molecular Dynamics [46] and Elastic Network Model [47].

4. Results and discussions

Figure 1 shows neutral particle production rates as a function of relative energy in collision of electrons with singly protonated

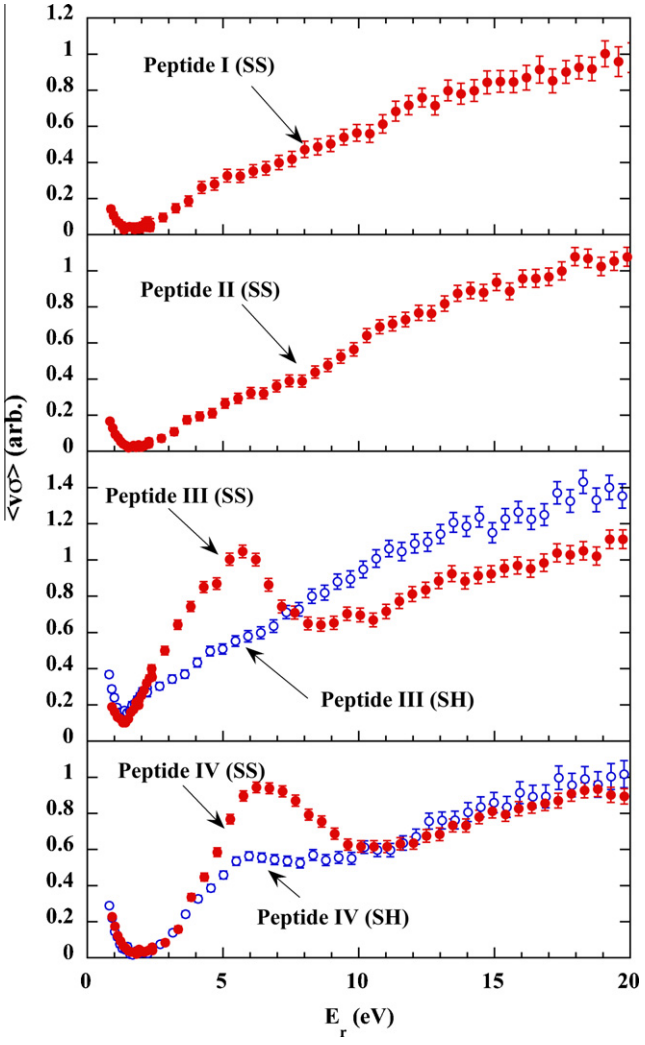

Figure 1. Neutral-particle production rate as a function of relative energies in collision of electrons with protonated mono-cations of Peptide I–IV (SS) (shown in Table 1). For Peptides III and IV (SS), results for the corresponding SH peptides are also compared.

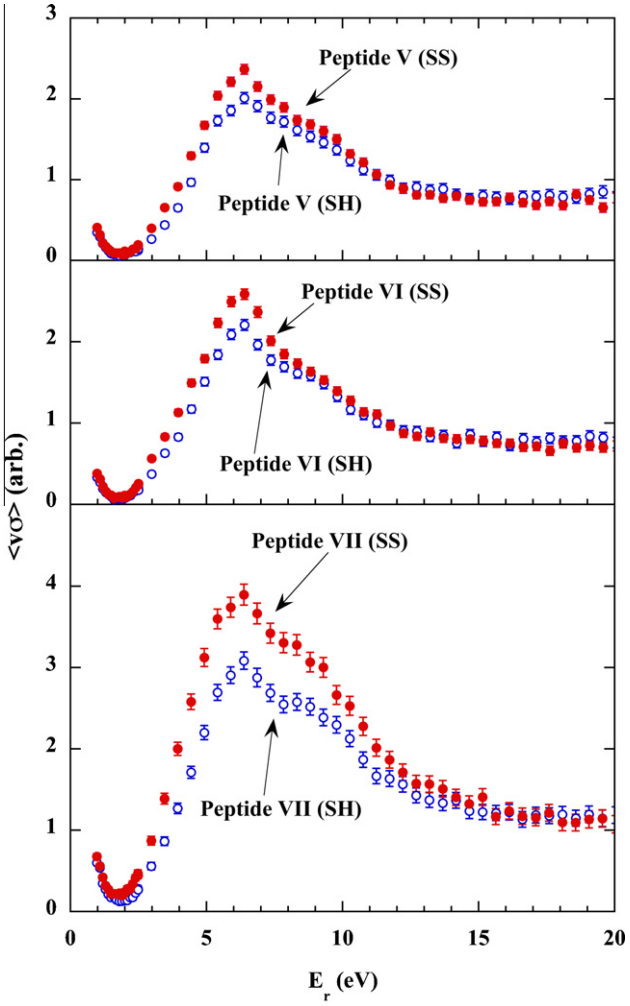

Figure 2. Neutral-particle production rate as a function of relative energies in collision of electrons with protonated mono-cations of Peptide V–VII (SS) (shown in Table 1). Results for the corresponding SH peptides are also compared.

Peptide I–IV. As can be seen in the figure, the rates increase toward zero energy, which represents well-known ECD process. Present experimental condition however did not allow to measure the rate at low energies, because the electron beam intensity decreases at the energies less than about 1 eV. The rates for the Peptide I (SS) and II (SS) consisting of two amino-acid residues increase only monotonically with energy. On the other hand, the rate for the Peptide III (SS) with a disulfide linkage shows a bump at around 6 eV. In order to study the origin of this bump, we performed the same measurements for the Peptide III (SH) which does not have an S–S bond: there is no bump for this ion (see Figure 1). That means the bump closely correlates with the disulfide bond. We extended the same measurements to the Peptide IV (SH) consisting of three amino-acid residues. As can be seen in Figure 1, there is a broad bump, which is the same as those observed previously for several peptides without S–S bond [38] and is deduced to come from the cleavage of peptide backbones. This bump is enhanced with the S–S linked Peptide IV (SS). Here, a question arises why bumps appear for the Peptide III (SS) and IV (SS) and do not occur for the Peptide I (SS) and II (SS) despite the presence of the disulfide bonds. A difference between them is that, for the Peptide III and IV, amino-acid residues rich in π–electron density such as Tyr and Glu are linked to Cys, respectively, while the Peptide I and II have no such amino-acid residues. Similarly, in the DR of $CH_3SSHCH_3^+$ studied with a storage-ring [32], no high-energy structure was observed in the cross sections for collision energies up to 16 eV, although high rates were observed around zero collision energies. This also supports our view, because the above ion lacks additional π–electron-rich amino-acid residues as well.

We have also extended the measurements to the peptides with internal S–S bonds. Figure 2 shows the neutral particle production rates in collisions of electrons with singly protonated Peptide V–VII consisting of nine amino-acid residues with and without S–S bond. As can be seen in the figure, resonant bumps appear at almost the same energies, which correspond to our previous results [38]. The addition of the S–S bond clearly enhances the rates. In these peptides, one of the cysteines also links to Tyr which is rich in π–electrons. To confirm the effect of Tyr, we performed the same experiments on 9-mer peptides with no Tyr next to Cys: 'Brain-binding': (sequence: Cys-Leu-Ser-Ser-Arg-Leu-Asp-Ala-Cys) and 'Conopressin S' (sequence: Cys-Ile-Ile-Arg-Asn-Cys-Pro-Lys-Gly-NH_2). The corresponding results are depicted in Figure 3 and, as anticipated, reveal even a clear decrease in the 'Brain-binding' bump heights for the SS peptides in comparison with those for the SH peptides, whereas some increase can be seen for the Conopressin S. Indeed, whereas the latter is possessed of the π–electron-containing Asn residue just near one of the Cys-moieties, the former has none of such side-chains in the proximity to Cys.

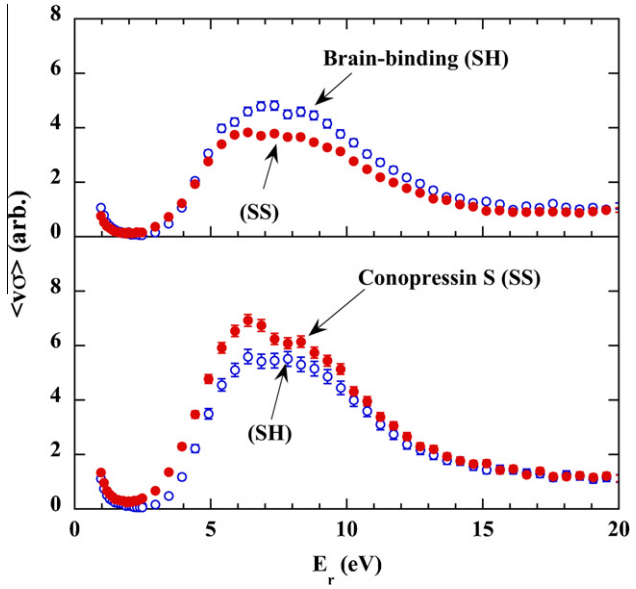

Figure 3. Neutral-particle production rate as a function of relative energies in collision of electrons with protonated mono-cations of 'Brain-binding' (SS) (sequence: Cys-Leu-Ser-Ser-Arg-Leu-Asp-Ala-Cys) and 'Conopressin S' (SS) (sequence: Cys-Ile-Ile-Arg-Asn-Cys-Pro-Lys-Gly-NH_2). Results for the corresponding SH peptides are also compared.

Another feature is that the bump heights are almost the same for the Peptide V and VI, while it is much larger for the Peptide VII.

To peform theoretical studies, the initial structures of OXT and VP were obtained from the PDB files available from the Protein Data Bank [PDB ID: 1NPO (OXT) and 1YF4 (VP)]. Because there is no PDB structure for VT, the initial structure of VT was obtained by the amino-acid mutation of OXT. For the convenience of classical molecular mechanics (MM) modeling, the NH_2 group was not added to the C-terminal of OXT, VP and VT, unlike in the actual compounds involved (it is known that the exact chemical nature of the C-cap is not very important for the actual oligopeptide conformation [48]). In order to make the protonated structure of OXT, a proton was added to the NH_2 group of its N-terminal, whereas VT and VP may anyway be considered monocations due to their positively charged Arg 8 residue (without protonating their N and/or C termini). Still, we have also protonated the C and N termini of the VP and VT to check, how protonation might affect the over-all conformation of these very short oligopeptides (the doubly protonated species were not used in the subsequent MM analysis). The idea was to make sure that our conclusions for the protonated molecules would apply to their electroneutral counterparts as well. Besides, our detailed DFT studies have shown that protonation does not seem to significantly affect the conformations and the S–S bond length of the oligopeptides under study (only the local conformations at the C-termini get noticeably changed, see, Figure 4, for example). Hence, we may in general apply our reasoning below to the responses of both protonated and non-protonated species to the incident electron attachment.

In analyzing pairwise amino-acid residue correlations along the MD trajectories, we have revealed several collective conformationally active motions in the oligomers. To this end, if we take into account only the dynamics of the 'rigid' amino-acid residues, i.e., just the dynamics of their centers of mass in the 3-D Cartesian space, then we obviously deal with the $3N - 6$ intra-molecular normal modes (N is the number of monomers in an oligopeptide). E.g., a typical 'rigid' nonapeptide should have 21 normal modes in total.

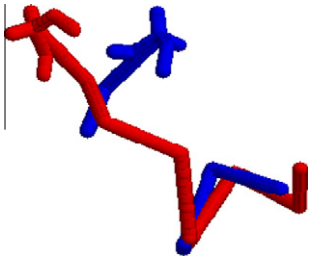

Figure 4. Superposition of the C-α-backbone conformations for the OXT oligopeptide with protonated N-terminus (red) and non-protonated N-terminus (blue). Only the Gly 9 residues of the both OXT forms are shown here in the all-atom 'stick' representation.

Our analysis shows, how many (and which) of these modes may definitely contribute to the collective motion, namely: seven modes for OXT, six modes for VP and five modes for VT. Thus, the MD trajectory simulated here represents collective modes to 88% for OXT, whereas those for VP and VT – only to 77%, with the rest of the dynamics belonging to the conventional chaotic thermal motion. In principle, our method is even capable of exploring the nonlinearity of the collective molecular dynamics, in that the correlations between the collective modes thus revealed can be estimated. Meanwhile, in OXT, VP and VT there are no additional correlations between the collective normal modes.

Finally, the most influential collective mode in OXT includes 3-D dynamics of the Ile 3 residue in X-, Y- and Z-directions in connection with different (X or Y or Z) 1-D dynamics of all other OXT residues. This is not the case either for VP or for VT.

Bearing all the above findings in mind, one may also notice a clear-cut correlation between the height of the experimentally observed bumps and the number/nature of the conformationally active collective modes in OXT, VP and VT. Indeed, the higher Feshbach resonance peak for OXT, in comparison to VP and VT (see Figure 2), readily associates with the higher content of collective motion in the over-all molecular dynamics of the OXT, as well as the presence of normal modes of special sort (including a dynamical 'guiding center' [49]: in our case the latter is correspondent to a relatively slow center-of-mass dynamics of some special amino-acid residue, the dynamical 'guiding center', bringing the centers of mass of all other residues in some very specific positions). Interestingly, the experimentally observed bump of VP is slightly higher than that of VT, which could also be attributed to the difference in the number of the principal collective modes in these oligopeptides. In our previous work on various peptides and nucleotides (see Ref. [37,50] and the references therein), we have suggested an interconnection between the incident electron attachment and cooperative effects in the electron structure (in particular, the creation of a resonant electron–hole pair – a charge transfer exciton – in protonated species). Our present results show that particular collective modes ought to be non-negligibly coupled with the cooperative electronic processes accompanying the incident electron attachment. Such modes should definitely be conformationally active.

The latter tentative conclusion is in full accord with the theoretical findings of the works [31], which advocates a conformationally dependent mechanism of the S–S-bond scission. Indeed, our experimental approach ought to allow us obtaining direct information about the molecular geometric cross-section. However, this should not be understood in the 'frozen, static geometry' sense. As our MD studies show, the peptide conformation should instead be considered as resulting from a kind of keenly balanced superposition of different molecular vibrational normal modes. Thus, our observation that the effect of the S–S-bridge is relatively small in some

of the longer oligopeptides under study should not be taken as paradoxical.

5. Conclusions

Resonant neutral particle emissions were observed at the collision energies of 6–7 eV in collisions of electrons with the peptide mono-cations with internal or external disulfide bonds, which are almost the same as those for the peptides without disulfide bonds. The appearance of these bumps depends on kinds of the amino-acid residues adjacent to Cys. It is deduced that π–electrons in such amino-acid residues correlate with the resonant excitation of core electrons resulting in high rates of electron capture and dissociation. In the longer oligopeptide bond-scission mechanisms, particular vibrational normal modes ought to play a very important role.

Acknowledgements

The experiment was supported by KAKENHI (Grant-in-Aid for Scientific Research) (20612019). JS and WW acknowledge support of the Deutsche Forschungsgemeinschaft through a grant to the Center for Functional Nanostructures (C5.1) and grant WE1863/17-2. GC acknowledges support from Deutsche Forschungsgemeinschaft (DFG) within the Priority Program 1243 'Quantum transport at the molecular scale' under contract CU 44/5-2, and by the European Union under contract IST-029192-2 'DNA-based nanoelectronic devices', the WCU (World Class University) program sponsored by the South Korean Ministry of Education, Science, and Technology Program (Project No. R31-2008-000-10100-0) and POSTECH, as well as the Center for Information Services and High Performance Computing (ZIH) at the Dresden University of Technology for computational resources. The work of SM and NK was supported in part by the research grants from Murata Science Foundation, Iketani Science and Technology Foundation.

References

[1] D. Zajfman, J.B.A. Mitchell, D. Schwalm, B.R. Rowe (Eds.), Dissociative Recombination, World Scientific, Singapore, 1995.
[2] M. Larsson, J.B.A. Mitchell, I.F. Schneider (Eds.), Dissociative Recombination, World Scientific, Singapore, 1999.
[3] R.A. Zubarev, N.L. Kelleher, F.W. McLafferty, J. Am. Chem. Soc. 120 (1998) 3265.
[4] R.A. Zubarev, N.A. Kruger, E.K. Fridriksson, M.A. Lewis, D.M. Horn, B.K. Carpenter, F.W. McLafferty, J. Am. Chem. Soc. 121 (1999) 2857.
[5] R.A. Zubarev et al., Anal. Chem. 72 (2000) 563.
[6] F. Kjeldsen, K.F. Haselmann, B.A. Budnik, F. Jensen, R.A. Zubarev, Chem. Phys. Lett. 356 (2002) 201.
[7] F. Kjeldsen, K.F. Haselmann, E.S. Sørensen, R.A. Zubarev, Anal. Chem. 75 (2003) 1267.
[8] R.A. Zubarev, Mass Spectrom. Rev. 22 (2003) 57.
[9] P.A. Chrisman, S.J. Pitteri, J.M. Hogan, S.A. McLuckey, J. Am. Soc. Mass Spectrom. 16 (2005) 1020.
[10] H.P. Gunawardena, M. He, P.A. Chrisman, S.J. Pitteri, J.M. Hogan, B.D.M. Hodges, S.A. McLuckey, J. Am. Chem. Soc. 127 (2005) 12627.
[11] J. Simons, Chem. Phys. Lett. 484 (2010) 81.
[12] A. Sawicka, P. Skurski, R.R. Hudgins, J. Simons, J. Phys. Chem. B 107 (2003) 13505.
[13] M. Sobczyk, J. Simons, J. Phys. Chem. B 110 (2006) 7519.
[14] I. Anusiewicz, J. Berdys-Kochanska, P. Skurski, J. Simons, J. Phys. Chem. A 110 (2006) 1261.
[15] I. Anusiewicz, J. Berdys-Kochanska, J. Simons, J. Phys. Chem. A 109 (2005) 5801.
[16] M. Sobczyk, I. Anusiewicz, J. Berdys-Kochanska, A. Sawicka, P. Skurski, J. Simons, J. Phys. Chem. A 109 (2005) 250.
[17] M. Sobczyk, D. Neff, J. Simons, Int. J. Mass Spectrom. 269 (2008) 149.
[18] P. Skurski, M. Sobczyk, J. Jakowski, J. Simons, Int. J. Mass Spectrom. 265 (2007) 197.
[19] M. Sobczyk, J. Simons, Int. J. Mass Spectrom. 253 (2006) 274.
[20] A. Sawicka, J. Berdys-Kochanska, P. Skurski, J. Simons, Int. J. Quantum Chem. 102 (2005) 838.
[21] F. Tureczek, M. Poláczek, A.J. Frank, M. Sadílek, J. Am. Chem. Soc. 122 (2000) 2361.
[22] F. Tureczek, J. Am. Chem. Soc. 125 (2003) 5954.
[23] G. Frison, G. van der Rest, F. Tureczek, T. Besson, J. Lemaire, P. Maître, J. Chamot-Rooke, J. Am. Chem. Soc. 130 (2008) 14916.
[24] E.A. Syrstad, D.D. Stephens, F. Tureczek, J. Phys. Chem. A 107 (2003) 115.
[25] E.A. Syrstad, F. Tureczek, J. Phys. Chem. A 105 (2001) 11144.
[26] F. Tureczek, X. Chen, C. Hao, J. Am. Chem. Soc. 130 (2008) 8818.
[27] R.D. Leib, W.A. Donald, M.F. Bush, J.T. O'Brien, E.R. Williams, J. Am. Chem. Soc. 129 (2007) 4894.
[28] E.W. Robinson, R.D. Leib, E.R. Williams, J. Am. Soc. Mass Spectrom. 17 (2006) 1469.
[29] R.D. Leib, W.A. Donald, M.F. Bush, J.T. O'Brien, E.R. Williams, J. Am. Soc. Mass Spectrom. 18 (2007) 1217.
[30] A.T. Iavarone, K. Paech, E.R. Williams, Anal. Chem. 76 (2004) 2231.
[31] E. Uggerud, Int. J. Mass Spectrom. 234 (2004) 45.
[32] A. Al-Khalili et al., J. Chem. Phys. 121 (2004) 5700.
[33] P. Hvelplund, B. Liu, S.B. Nielsen, S. Tomita, Int. J. Mass Spectrom. 225 (2003) 83.
[34] T. Chakraborty, A.I.S. Holm, P. Hvelplund, S.B. Nielsen, J.-C. Poully, E.S. Worm, E.R. Williams, J. Am. Soc. Mass Spectrom. 17 (2006) 1675.
[35] R.R. Hudgins, K. Håkansson, J.P. Quinn, C.L. Hendrickson, A.G. Marshall, in: Proc. 50th ASMS Conference on Mass Spectrometry and Allied Topics, Orlando, FL, 2002.
[36] S. Tsuzuki, M. Yoshida, T. Uchimaru, M. Mikami, J. Phys. Chem. A 105 (2001) 769.
[37] T. Tanabe, E.B. Starikov, K. Noda, Chem. Phys. Lett. 449 (2007) 202.
[38] T. Tanabe, K. Noda, M. Saito, S. Lee, Y. Ito, H. Takagi, Phys. Rev. Lett. 90 (2003) 193201.
[39] T. Tanabe, K. Noda, Nucl. Instrum. Methods A 496 (2003) 233.
[40] T. Tanabe, K. Chida, K. Noda, I. Watanabe, Nucl. Instrum. Methods A 482 (2002) 595.
[41] T. Tanabe, K. Noda, E. Syresin, Nucl. Instrum. Methods A 532 (2004) 105.
[42] M.J. Frisch et al., GAUSSIAN 03, Revision D.01, GAUSSIAN, Inc., Pittsburgh, PA, 2003.
[43] D.A. Case et al., AMBER 10, University of California, San Francisco, CA, 2008.
[44] V. Hornak, R. Abel, A. Okur, B. Strockbine, A. Roitberg, C. Simmerling, Proteins 65 (2006) 712.
[45] E.B. Starikov, K. Bräsicke, E.W. Knapp, W. Saenger, Chem. Phys. Lett. 336 (2001) 504.
[46] A. Amadei, A.B.M. Linssen, H.J.C. Berendsen, Proteins 17 (1993) 412.
[47] P. Durand, G. Trinquier, Y.H. Sanejouand, Biopolymers 34 (1994) 759.
[48] A.J. Doig, R.L. Baldwin, Protein Sci. 4 (1995) 1325.
[49] P. Ghendrih, R. Lima, R.V. Mendes, J. Phys. A: Math. Theor. 41 (2008) 465501.
[50] T. Tanabe, E.B. Starikov, K. Noda, Chem. Phys. Lett. 467 (2008) 154.